

PAPER

# Controlling the optical properties of monocrystalline 3C-SiC heteroepitaxially grown on silicon at low temperatures

To cite this article: Gerard Colston and Maksym Myronov 2017 *Semicond. Sci. Technol.* **32** 114005

View the [article online](#) for updates and enhancements.

## Related content

- [Quantum dot optoelectronic devices: lasers, photodetectors and solar cells](#)  
Jiang Wu, Siming Chen, Alwyn Seeds et al.
- [Epitaxial graphene formation on 3C-SiC/Si thin films](#)  
Maki Suemitsu, Sai Jiao, Hirokazu Fukidome et al.
- [Metal organic vapour phase epitaxy](#)  
Pierre Gibart

# Controlling the optical properties of monocrystalline 3C-SiC heteroepitaxially grown on silicon at low temperatures

Gerard Colston<sup>1</sup> and Maksym Myronov<sup>1</sup>

Department of Physics, The University of Warwick, Gibbet Hill Road, Coventry, CV4 7AL, United Kingdom

E-mail: [g.colston@warwick.ac.uk](mailto:g.colston@warwick.ac.uk) and [M.Myronov@warwick.ac.uk](mailto:M.Myronov@warwick.ac.uk)

Received 15 June 2017, revised 22 August 2017

Accepted for publication 8 September 2017

Published 4 October 2017



## Abstract

Cubic silicon carbide (3C-SiC) offers an alternative wide bandgap semiconductor to conventional materials such as hexagonal silicon carbide (4H-SiC) or gallium nitride (GaN) for the detection of UV light and can offer a closely lattice matched virtual substrate for subsequent GaN heteroepitaxy. As 3C-SiC can be heteroepitaxially grown on silicon (Si) substrates its optical properties can be manipulated by controlling the thickness and doping concentrations. The optical properties of 3C-SiC epilayers have been characterized by measuring the transmission of light through suspended membranes. Decreasing the thickness of the 3C-SiC epilayers is shown to shift the absorbance edge to lower wavelengths, a result of the indirect bandgap nature of silicon carbide. This property, among others, can be exploited to fabricate very low-cost, tuneable 3C-SiC based UV photodetectors. This study investigates the effect of thickness and doping concentration on the optical properties of 3C-SiC epilayers grown at low temperatures by a standard Si based growth process. The results demonstrate the potential photonic applications of 3C-SiC and its heterogeneous integration into the Si industry.

Keywords: 3C-SiC, optical, CVD, epitaxy, photodetector, virtual substrate, transmission

(Some figures may appear in colour only in the online journal)

## 1. Introduction

Ultraviolet (UV) photodetectors have many applications in the industrial sector, environmental sensing and safety. UV sensing can offer better efficiency in curing and sterilization processes as well as protect humans from the damaging effects of prolonged exposure to radiation from the Sun. Low-cost UV sensors would satisfy a large demand from various sectors. Due to its low-cost and scalability, silicon (Si) is often considered as a material for UV photodiodes, however, Si detectors are limited in operating temperature, are not solar blind and can be degraded by constant exposure to UV radiation, decreasing device sensitivity and increasing noise [1, 2].

Silicon carbide (SiC) is a wide bandgap compound semiconductor which is an excellent material for UV photodetectors in terms of its ability to operate in harsh environments and withstand the damaging effects of ionizing radiation [3, 4]. SiC can be formed in various crystalline states, known as polytypes. All of them exhibit an indirect energy bandgap, see figure 1. In case of 3C-SiC the indirect energy band gap at the *X* point is  $\sim 2.4$  eV (520 nm) while the direct one at the  $\Gamma$  point is  $\sim 6$  eV (205 nm).

For bulk materials operating at room temperature or above, optical absorption occurs as long as the incident light exceeds this bandgap due to the addition of momentum transfer from phonons within the crystal leading to indirect transitions. However, the cubic polytype, 3C-SiC, can be heteroepitaxially grown on Si substrates to controllable thicknesses which can manipulate the nature of phonon assisted light absorption in the material. In addition, the

<sup>1</sup> Authors to whom any correspondence should be addressed.

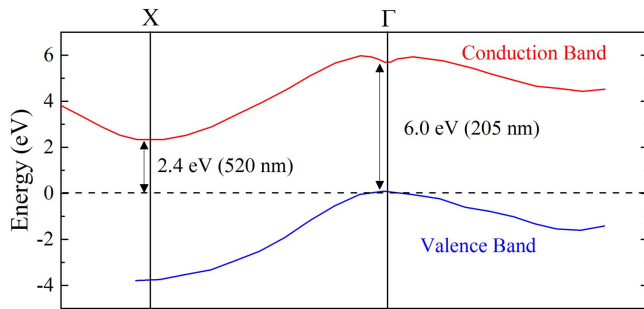


**Figure 1.** Simplified band structure of 3C-SiC semiconductor at room-temperature.

inclusion of impurities in the epilayer can also be used to affect the absorption of UV light within semiconductor films. Tunable photodetectors have been demonstrated with III–V ternary alloys such as aluminium gallium nitride (AlGaIn) by controlling the Al impurity concentration to manipulate the bandgap of the material [5]. One of the downsides to III–V based semiconductors is that they cannot be grown within Si based growth processes which means that heterogeneous integration of wide bandgap III–Vs with Si can only really be achieved using devices on separate chips or wafer bonding techniques. 3C-SiC has the potential to integrate a wide bandgap semiconductor material with Si growth technology, however, thus far the high quality growth of 3C-SiC has relied on ‘hot-wall’ reactors dedicated to SiC epitaxy which increases growth costs. Recently, it was demonstrated that high quality 3C-SiC/Si epi wafers could be grown using an industrial standard Si based ‘cold-wall’ reduced pressure chemical vapour deposition (RP-CVD) system [6]. As well as offering greater flexibility to device design, 3C-SiC/Si based devices can significantly reduce the cost of UV photodiodes compared to those fabricated purely from hexagonal silicon carbide (4H-SiC or 6H-SiC) or GaN based compounds.

Another potential application of 3C-SiC that has attracted attention in previous years is as a virtual substrate for the heteroepitaxy of the compound semiconductor GaN for LED, radio frequency RF communications and power electronic applications. GaN has a direct bandgap of  $\sim 3.4$  eV (365 nm). 3C-SiC offers an advantage for GaN epitaxy as the lattice mismatch between the two materials is lower ( $\sim 3.5\%$ ), comparing to Si ( $\sim 17\%$ ), but allows the incorporation of GaN on a Si substrate. In addition, 3C-SiC offers the unique advantage that it can be grown on both the (111) and (001) crystal orientations, providing ideal templates for the growth of hexagonal and cubic GaN respectively. Cubic GaN in particular is of interest as it can increase efficiency of green LEDs overcoming the *droop effect* typically observed at green wavelengths in GaN based ternary compounds [7]. GaN LEDs are often fabricated using a *flip-chip* technique to increase heat dissipation and efficiency, in which the light is emitted from the underside of the GaN epilayers, typically through the sapphire substrate [8]. In order for 3C-SiC/Si to replace sapphire in the LED industry and minimise disruption to device architecture, it would be beneficial if the 3C-SiC was optically transparent to the emitted wavelengths from UV

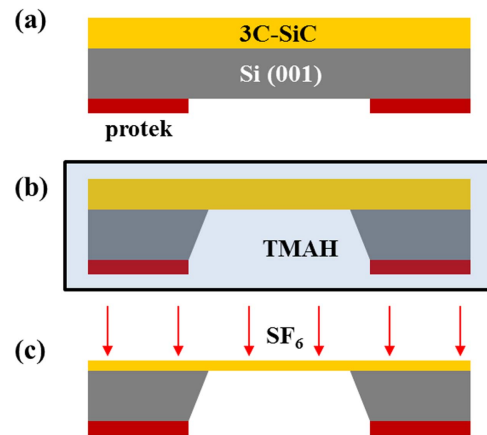


**Figure 2.** 3C-SiC membrane fabrication process: (a) the underside of the Si substrate is selectively patterned with the photoresist ProTEK PSB by photolithography (b) Si is selectively etched in TMAH at  $90^\circ\text{C}$  for approximately 14 h (c) for thickness variation the 3C-SiC film was dry etched for varying durations within a reactive ion etch of  $\text{SF}_6$ .

to green (200–550 nm). During device fabrication, the Si substrate can easily be removed by chemical wet etching while leaving the 3C-SiC epilayer intact as a protective coating for the GaN, providing it does not absorb light emitted from the GaN LED. Even relatively thin 3C-SiC buffer layers of  $\sim 700$  nm have been shown to improve LED performance by more than doubling the output intensity [9]. Also, GaN heteroepitaxy on the same 3C-SiC/Si substrates would enable the creation of new multi junction photodetectors with enhanced and improved light absorption in the UV spectrum.

In this study, the dependence of 3C-SiC epilayer thickness and doping concentrations on light absorption has been investigated as a first step towards a low-cost, tuneable 3C-SiC UV photodetector and determining the optimal buffer layer thickness for optical transmission from GaN based LEDs.

## 2. Experimental details

3C-SiC epilayers were grown at low temperatures by RP-CVD within an ASM Epsilon 2000 single wafer, ‘cold wall’ quartz chamber system at a growth temperature of equal or below  $1200^\circ\text{C}$  [6]. For thickness dependency measurements, a single epilayer  $\sim 1.2\ \mu\text{m}$  was grown and thinned post-growth. The epilayer was grown on a standard on axis Si (001) substrate of  $\sim 525\ \mu\text{m}$  thickness and 100 mm diameter.

Optical transmission measurements were carried out through suspended 3C-SiC square membranes fabricated by anisotropic etching within tetramethylammonium hydroxide (TMAH), see figure 2. The alkaline resistant photoresist ProTEK PSB was spun onto the backside of the Si substrate and patterned into squares of  $\sim 2$  mm side length using UV photolithography. To reduce the thickness of the 3C-SiC membranes, the  $1.2\ \mu\text{m}$  thick epilayer was thinned using dry etching within a reactive ion etch system using  $\text{SF}_6$  and  $\text{O}_2$

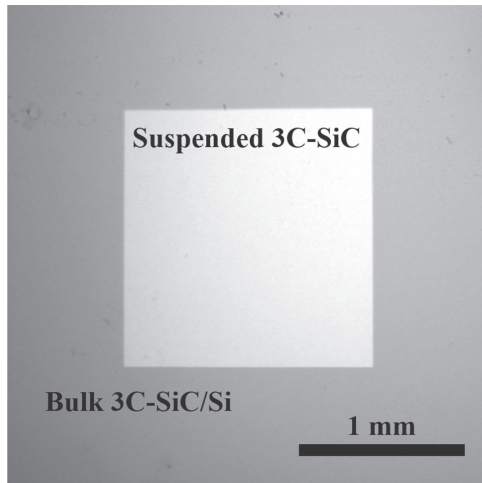


**Figure 3.** Optical image of a suspended, square 3C-SiC membrane with side lengths of  $\sim 1.5$  mm.

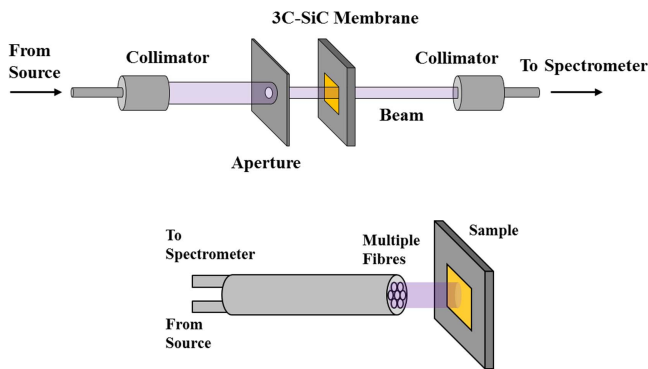


**Figure 4.** Top—Experimental set-up for transmission measurements. Collimators were used to focus the beam through an aperture which limited the beam spot size such that it could pass through a 3C-SiC membrane. Bottom—Experimental set-up for reflectivity measurements. A multi fibred optical cable was used to both transmit and receive the beam.

gases. Thinning the 3C-SiC in this manner allows more parameters of the epilayers such as doping and surface roughness to be kept relatively constant, opposed to growing multiple layers.

The use of suspended membranes allows true absorption measurements of suspended epilayers to be made without having to consider the impact of the epilayer/substrate interface and Si substrate itself [10]. Optical transmission measurements were carried out at room-temperature by placing the suspended membranes (figure 3) in the path of a beam of light produced by a tungsten and deuterium lamp with wavelength of 200–1000 nm, see figure 4. The transmitted beam of light was measured using a Si based spectrometer capable of measuring intensity as a function of wavelength.

The effect of doping was also investigated on suspended 3C-SiC structures by growing a  $\sim 50$  nm thick, phosphorus (P) doped (n-type) capping epilayer on the surface of a 300 nm thick intrinsic 3C-SiC buffer, see figure 5. Extremely high levels of P doping in the range of  $1 \times 10^{19} - 5 \times 10^{20} \text{ cm}^{-3}$  have been demonstrated, measured using

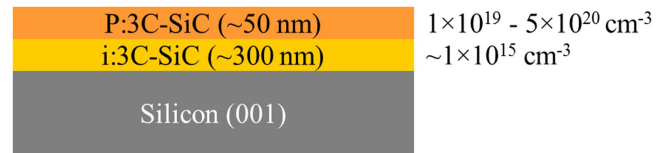


**Figure 5.** Doped 3C-SiC heterostructure cross sectional schematic.

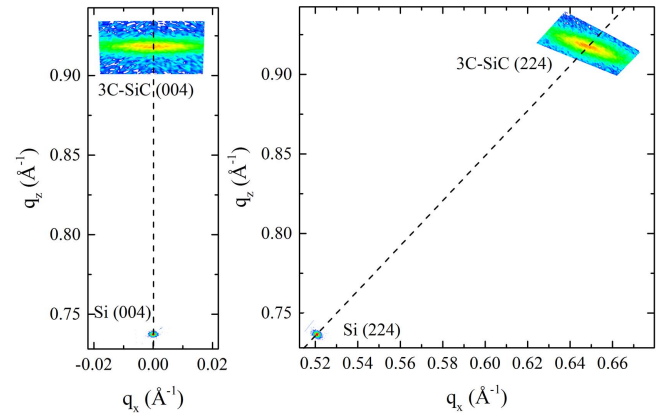


**Figure 6.** Symmetric and asymmetric RSMs of the  $1.2 \mu\text{m}$  thick 3C-SiC epilayer. The dashed lines indicate the expected Bragg peak positions of epilayers that are free of tilt and fully relaxed with respect to the Si substrate in the symmetric and asymmetric RSMs respectively.

secondary ion mass spectroscopy (SIMS) measurements carried out by Evans Analytical Group and confirmed to be between 50% and 100% electrically active through Hall effect measurements, results not shown here. The 300 nm buffer was introduced for two reasons, firstly it increases the quality of the 3C-SiC by allowing most of the stacking faults and other defects to annihilate before the doped epilayer was grown and it also prevents the intermixing of dopants within the Si substrate.

Suspended membranes were fabricated, using the process previously described, from this new material and used to investigate the effect of the doping on the optical properties of the 3C-SiC.

### 3. Results and discussions

The as-grown 3C-SiC epilayers were found to be mono-crystalline, free of tilt and almost fully relaxed with only slight residual tensile strain. These parameters were analysed using high resolution x-ray diffraction techniques and symmetric and asymmetric reciprocal space maps (RSMs) can be seen in figure 6. RSMs were acquired using a lab based Panalytical X'Pert MRD diffractometer using  $\text{Cu K}\alpha_1$  radiation.

The presence of slight residual strain in the 3C-SiC epilayer is a result of the thermal mismatch between the two epilayers, however, this strain allows the fabrication of suspended membranes without the 3C-SiC films collapsing on themselves. The surface morphology of the 3C-SiC epilayers was characterized by atomic force microscopy (AFM) in

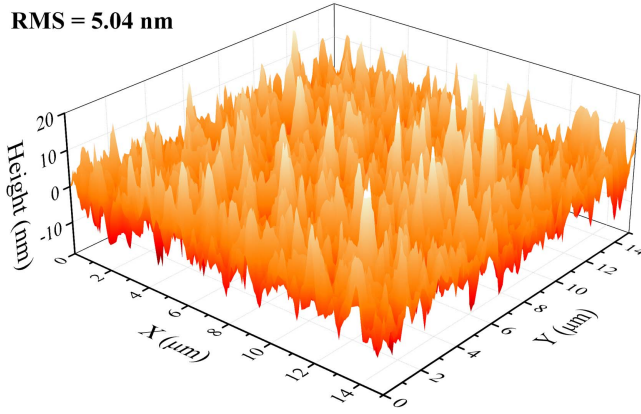


**Figure 7.** Atomic force microscopy (AFM) map of the 3C-SiC surface morphology, acquired in tapping mode, using  $\text{Si}_3\text{N}_4$  tips.

tapping mode using a Veeco Multimode AFM with  $\text{Si}_3\text{N}_4$  tips to capture the surface profile. A typical  $15 \times 15 \mu\text{m}^2$  is shown in figure 6. The surface roughness of the  $1.2 \mu\text{m}$  thick 3C-SiC epilayer was found to be  $\sim 5 \text{ nm}$  offering a relatively smooth and mirror like epilayer surface which helps to reduce any unwanted scattering of light through the membranes, see figure 7.

The optical transmission of light through the suspended membranes leads to fringes in the spectra due to the interference of light within the epilayer. This allows accurate thickness measurements of the 3C-SiC membranes as constructive interference fringes will occur at positions defined by

$$m\lambda = 2n_{3C}(\lambda)d, \quad (1)$$

where  $m$  is an integer value,  $n_{3C}(\lambda)$  is the refractive index of light through 3C-SiC for a specific wavelength ( $\lambda$ ). Mapping the positions of these fringes allows one to extract thickness, assuming the refractive index of the 3C-SiC is known as a function of wavelength.

### 3.1. Effect of epilayer thickness

The transmission of light was measured through membranes of thicknesses ranging from 130 to 1270 nm, see figure 8. As the thickness of the membranes decreases, the transmission of light at lower wavelengths increases.

The variation in the transmission at low wavelengths is shown in figure 9, where the wavelength at which  $<5\%$  of light is transmitted has been measured as a function of the membrane thickness. The value of 5% was chosen as certain thin samples exhibited complete absorption below the measurement threshold of the Si diode used in the optical measurements. An almost linear dependency is observed with the defined 5% cut-off wavelength implying that the absorption of light at these wavelengths is dominated by phonon assisted transitions which depend on the interaction volume of the thin film, hence the transmission decreases with thickness.

The reflectance spectrum was obtained for the sample of  $\sim 580 \text{ nm}$  thickness, see figure 10. Reflectance fringes align with the transmission signal. As the wavelength reduces, the reflectance signal decreases as it becomes dominated only by

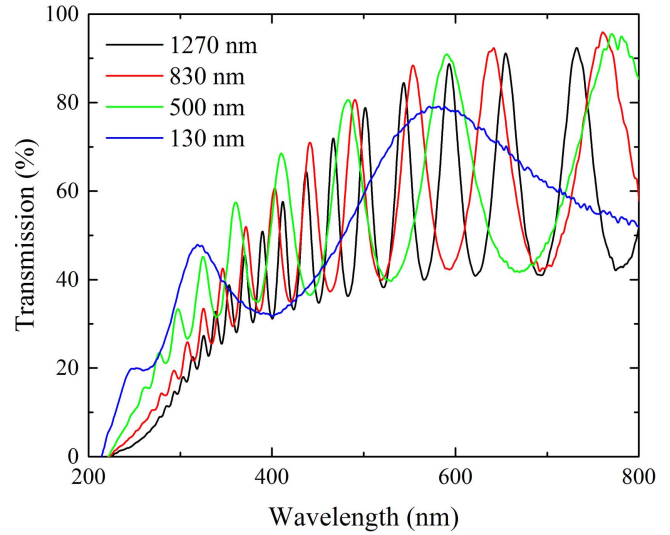


**Figure 8.** Transmission spectra through selected membranes of varying thickness.

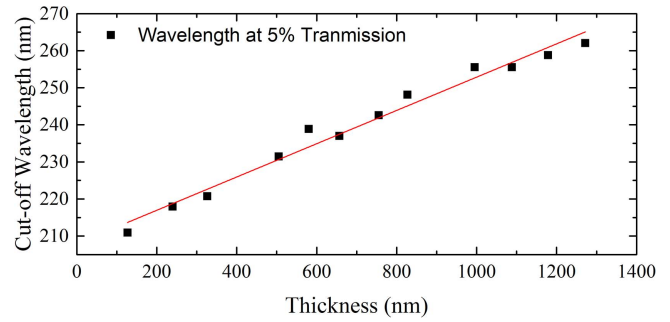


**Figure 9.** Wavelength at which below 5% of incident light is transmitted as a function of 3C-SiC thickness.

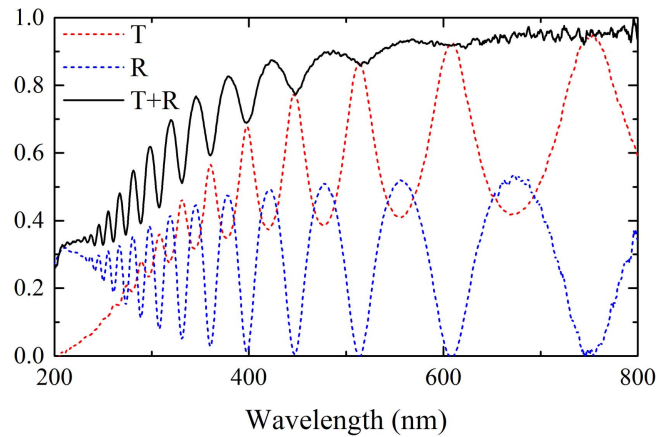


**Figure 10.** Transmission ( $T$ ) and reflectance ( $R$ ) coefficients of a  $580 \text{ nm}$  thick 3C-SiC suspended membrane.

the initial reflectance off the epilayer surface whereas at longer wavelengths the reflectance includes the signal due to reflection off the rear interface. The reflectance coefficient decreases to 0.3 at  $225 \text{ nm}$  wavelength which corresponds to a 3C-SiC refractive index of 3.58 using the Fresnel equation for



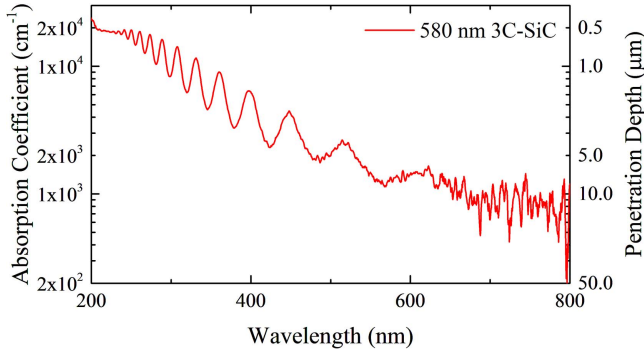


**Figure 11.** The attenuation coefficient and penetration depth for the 580 nm thick 3C-SiC epilayer as a function of wavelength.

reflectance given by

$$R = \left( \frac{n_1 - n_2}{n_1 + n_2} \right)^2. \quad (2)$$

Not being able to simultaneously measure the reflectance and transmission using this experimental set-up led to systematic errors between the two measurements as can be seen in figure 10 as  $T + R$  does not entirely eliminate the fringe effects. Another useful feature to note is that total light measured at long wavelengths is not equal to 100% indicating that some light may be being scattered by the non-uniform surface of the epilayers or that the crystalline defects within the 3C-SiC are introducing intermediate states within the bandgap that are enabling sub-gap absorption.

The value of  $T + R$  gives the total amount of light not absorbed through the sample, therefore the attenuation coefficient ( $\alpha$ ) can be determined using the approximate relationship

$$T + R = e^{-\alpha t}, \quad (3)$$

where  $t$  is the thickness of the sample. Using this value the penetration depth ( $\delta$ ) can be calculated using

$$\delta = \frac{1}{\alpha} \quad (4)$$

this is plotted in figure 11. The measured attenuation coefficient is only valid for short wavelengths where reflection interference patterns are not observed as equation (3) does not take into account light that is reflected back off the rear interface of the membrane which effectively increases the sample thickness and overestimates light absorption.

### 3.2. Effect of n-type doping

Transmission spectra were also obtained for heterostructures with high levels of n-type doping. The doping levels in the three heterostructures were determined through SIMS measurements, which calculated the levels of P and background N in the epilayers. A noticeable shift in the spectra at low wavelengths can be observed indicating that even the presence of a thin doped 3C-SiC epilayer within a larger heterostructure can have an effect on the absorption of light within the layer, see figure 12. The doped capping layer was maintained at 50 nm for two samples, however, the high level

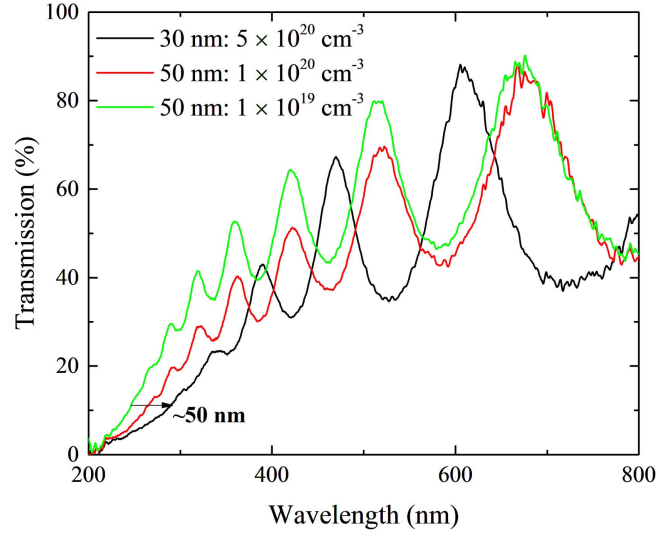


**Figure 12.** Transmission of light through 3C-SiC samples with capping layers of varying P doping concentrations.

of dopant incorporation in the highest doped sample led to a reduced thickness of 30 nm which causes the change in oscillation period. From previous results, a thinner epilayer would increase the transmission at low wavelengths, however, in this case the high level of doping continues to increase the optical absorption in the layer at short wavelengths. This is an important factor to be considered when designing a photosensitive 3C-SiC based device and could potentially influence the operation of other devices where highly doped regions of 3C-SiC are introduced to reduce contact resistance.

The origin of this shift in transmission spectra cannot be ascertained using the measurements carried out in this study. The incorporation of high levels of n-type dopants has been modelled to reduce the bandgap of 3C-SiC by  $\sim 200$  meV at doping levels of  $10^{20} \text{ cm}^{-3}$  which would increase optical absorption [11]. Alternatively, the presence of P in the band structure could offer intermediate states for electron excitation. As P is a shallow impurity in 3C-SiC, typically at around 48 meV from the conduction band the effect would only be subtle as shown in the presented results [12]. Either of these effects could explain the shift in the transmission data.

## 4. Conclusions

As silicon carbide is an indirect bandgap semiconductor its optical properties are highly dependent on its thickness. This property can be exploited in 3C-SiC as it can be epitaxially grown on Si substrates with precise control over properties such as thickness and doping. The results of this investigation demonstrate that 3C-SiC offers a route to tuneable UV photodetectors or can offer a protective coating on UV susceptible devices by simply manipulating the thickness and doping profile of the material. Using the novel 3C-SiC growth process invented by the authors at the University of Warwick, these results demonstrate that 3C-SiC can be integrated

directly with the growth of Si or other group IV semiconductors (SiGe, Ge, GeSn) for true heterogeneous integration of narrow and wide bandgap semiconductors on integrated circuits and devices. As a potential virtual substrate for GaN growth, traditional flip-chip fabrication techniques are not possible on bulk 4H-SiC without first removing the substrate, which is a challenge with SiC. However, fabricating GaN based LEDs on 3C-SiC offers an opportunity to emit light through the 3C-SiC without significant losses while the layer can also act as a mechanically robust, radiation resistant protective coating on the GaN device also acting as a diffusion barrier from foreign species. The results from this study suggest that for green wavelengths ( $\sim 550$  nm) 3C-SiC epilayers up to  $\sim 1$   $\mu\text{m}$  can transmit a significant proportion of light, while for blue wavelengths ( $\sim 400$  nm) and below the epilayer thickness will need to be reduced to allow such transmission. Another option is to reduce the doping concentration of the 3C-SiC as unintentional doping in the layers could lead to unwanted absorption and it is also speculated that the high density of defects in the 3C-SiC/Si interface could be leading to increased absorption at higher wavelengths. Removal of the Si substrate allows one to access and treat/etch away this defective region which could be a method to improve optical properties of these films.

As 3C-SiC can now be grown on silicon substrates using standard cold-wall based RP-CVD epitaxial processes, the material could potentially be grown on wafer diameters up to 300 mm and beyond. 3C-SiC offers an interesting material for photonic applications and the demonstrated epilayers will not only significantly reduce the cost of 3C-SiC based devices but also allow 3C-SiC to be integrated with other device structures that are commonly fabricated on Si substrates.

## Acknowledgments

This work was supported by the University of Warwick's Higher Education Innovation Fund (HEIF).

## References

- [1] Arp U *et al* 2005 Damage to solid-state photodiodes by vacuum ultraviolet radiation *J. Electron Spectrosc. Relat. Phenom.* **144** 1039
- [2] Esebamen O X 2016 Effect of UV radiation surface damage on silicon position sensitive photodetector *Optik* **127** 599
- [3] Hirabayashi Y *et al* 1994 Spectral response of a photodiode using 3C-SiC single-crystalline film *Sensors Actuators A* **43** 164
- [4] Nava F *et al* 2008 Silicon carbide and its use as a radiation detector material *Meas. Sci. Technol.* **19** 102001
- [5] Sandvik P *et al* 2001  $\text{Al}_x\text{Ga}_{1-x}\text{N}$  for solar-blind UV detectors *J. Cryst. Growth* **231** 366
- [6] Myronov M *et al* 2015 Growing epitaxial 3C-SiC on single-crystal silicon, GB1513014.9
- [7] Kim M H *et al* 2007 Origin of efficiency droop in GaN-based light-emitting diodes *Appl. Phys. Lett.* **91** 183507
- [8] Chang S J *et al* 2005 Nitride-based flip-chip ITO LEDs *IEEE Trans. Adv. Packag.* **28** 273
- [9] Zhu Y H *et al* 2009 Demonstration on GaN-based light-emitting diodes grown on 3C-SiC/Si(111) *J. Appl. Phys.* **106** 124506
- [10] Yamaguchi Y-i *et al* 1996 Properties of heteroepitaxial 3C-SiC films grown by LPCVD *Sensors Actuators A* **54** 695
- [11] Lindefelt U 1998 Doping-induced band edge displacements and band gap narrowing in 3C-, 4H-, 6H-SiC, and Si *J. Appl. Phys.* **84** 2628
- [12] Ivanov I G *et al* 2010 Ionization energy of the phosphorus donor in 3C-SiC from the donor-acceptor pair emission *J. Appl. Phys.* **108** 063532